

## First results of the Lomonosov TUS and GRB experiments

S.V. Biktemerova<sup>b</sup>, A.V. Bogomolov<sup>a</sup>, V.V. Bogomolov<sup>a</sup>, A.A. Botvinko<sup>c</sup>, A.J. Castro-Tirado<sup>d</sup>,  
 E.S. Gorbovskoy<sup>a</sup>, N.P. Chirskaya<sup>a</sup>, V.E. Ereemeev<sup>a</sup>, G.K. Garipov<sup>a</sup>, V.M. Grebenyuk<sup>b,e</sup>,  
 A.A. Grinyuk<sup>a</sup>, A.F. Iyudin<sup>a</sup>, S. Jeong<sup>f</sup>, H.M. Jeong<sup>f</sup>, N.L. Jioeva<sup>a</sup>, P.S. Kazarjan<sup>a</sup>, N.N. Kalmykov<sup>a</sup>,  
 M.A. Kaznacheeva<sup>a</sup>, B.A. Khrenov<sup>a</sup>, M.B. Kim<sup>f</sup>, P.A. Klimov<sup>a</sup>, E.A. Kuznetsova<sup>a</sup>, M.V. Lavrova<sup>a</sup>,  
 J. Lee<sup>f</sup>, V.M. Lipunov<sup>a</sup>, O. Martinez<sup>g</sup>, I.N. Mjagkova<sup>a</sup>, M.I. Panasyuk<sup>a</sup>, I.H. Park<sup>f</sup>, V.L. Petrov<sup>a</sup>,  
 E. Ponce<sup>g</sup>, A.E. Puchkov<sup>c</sup>, H. Salazar<sup>g</sup>, O.A. Saprykin<sup>c</sup>, A.N. Senkovsky<sup>c</sup>, S.A. Sharakin<sup>a</sup>,  
 A.V. Shirokov<sup>a</sup>, S.I. Svertilov<sup>a</sup>, A.V. Tkachenko<sup>b</sup>, L.G. Tkachev<sup>b,e</sup>, I.V. Yashin<sup>a</sup>, M.Yu. Zotov<sup>a</sup>

<sup>a</sup>Lomonosov Moscow State University, GSP-1, Leninskie Gory, Moscow, 119991, Russia

<sup>b</sup>Joint Institute for Nuclear Research, Joliot-Curie, 6, Dubna, Moscow region, Russia, 141980

<sup>c</sup>Space Regatta Consortium, ul. Lenina, 4a, 141070 Korolev, Moscow region, Russia

<sup>d</sup>Instituto de Astrofísica de Andalucía (IAA-CSIC), P.O.Box 03004, E-18080 Granada, Spain

<sup>e</sup>Dubna State University, University str., 19, Bld.1, Dubna, Moscow region, Russia

<sup>f</sup>Department of Physics and ISTS, Sungkyunkwan University, Seobu-ro 2066, Suwon, 440-746 Korea and

<sup>g</sup>Benemérita Universidad Autónoma de Puebla,

4 sur 104 Centro Histórico C.P. 72000, Puebla, Mexico

On April 28, 2016, the Lomonosov satellite, equipped with a number of scientific instruments, was launched into orbit. Here we present briefly some of the results obtained with the first orbital telescope of extreme energy cosmic rays TUS and by a group of detectors aimed at multi-messenger observations of gamma-ray bursts.

### I. INTRODUCTION

“Lomonosov” is an orbital scientific laboratory developed at Lomonosov Moscow State University in close collaboration with Joint Institute for Nuclear Research (Russia), University of California, Los Angeles (USA), Sungkyunkwan University (Republic of Korea), Benemérita Universidad Autónoma de Puebla (Mexico), Russian space industry organizations and a few other partners. The primary objectives of the Lomonosov mission include registration of:

- extreme energy cosmic rays (EECRs, energies above  $\sim 50$  EeV),
- gamma-ray bursts (GRBs) in visible, UV, gamma-, and X-rays,
- transient luminous events (TLEs) in the upper atmosphere,
- energetic trapped and precipitated radiation (electrons and protons) at a low-Earth orbit in connection with global geomagnetic disturbances.

To reach the goals, Lomonosov is equipped with a whole number of different instruments [1]. It was put into orbit on April 28, 2016, from the new Russian space launching site Vostochny. The satellite has a sun-synchronous orbit with an inclination of  $97^\circ 3$ , a period of  $\approx 94$  min, and a height of about 500 km.

In what follows, we briefly present some results obtained with the first orbital detector of EECRs, TUS, and a group of instruments aimed at detecting GRBs.

### II. RESULTS FROM TUS

TUS (Tracking Ultraviolet Set-up) is the first detector developed for registering extreme energy cosmic rays from space [2, 3]. It consists of two main parts: a parabolic mirror-concentrator of the Fresnel type and a square-shaped 256-pixel photodetector in the focal plane of the mirror. The mirror has an area of about  $2 \text{ m}^2$ . The field of view (FOV) equals approximately  $80 \text{ km} \times 80 \text{ km}$  at sea level with a spatial resolution of 5 km. Pixels of the TUS photodetector are photomultiplier tubes Hamamatsu R1463 with multialkali cathode of 13 mm diameter. The pixel wavelength band 240–400 nm is limited by a UV filter and by PMT quantum efficiency. Light guides with square entrance apertures ( $15 \text{ mm} \times 15 \text{ mm}$ ) and circular outputs are employed to fill uniformly the detector’s FOV.

The TUS electronics can operate in four modes intended for detecting various fast UV phenomena in the atmosphere at different time scales with different time sampling. The main mode is aimed at registering extensive air showers (EASs) born by EECRs and has a time sampling of  $0.8 \mu\text{s}$ . Two other modes have time sampling of  $25.6 \mu\text{s}$  and  $0.4 \text{ ms}$  for studying TLEs of different kinds slower than elves: sprites, blue jets, gigantic jets, etc. The fourth mode has a time sampling of  $6.6 \text{ ms}$  for detecting micro-meteors, space debris and thunderstorm activity at a longer time scale. In each mode, waveforms consist of 256 time samples. The trigger algorithm consists of two levels. The first level trigger decision is based on a comparison of fixed length sums of analog-to-digital converter (ADC) counts calculated for each pixel with a threshold level that depends on a similar value obtained for the background noise. At the second level

trigger, the geometry and number of hit pixels are analyzed. Accuracy of the trigger time stamps equals 1 s. TUS operates during nocturnal segments of the orbit.

All four modes were tested in the first months of operation. The main observational time was dedicated to the EAS mode. The measurements demonstrated an unexpectedly rich variety of UV radiation in the atmosphere, including anthropogenic and auroral lights, distant thunderstorm effects, etc., which considerably limit time for EAS observations. In what follows, we present a few examples of different phenomena registered with TUS.

More than 80% of all TUS records consist of noise-like events that are likely to be caused by random fluctuations of the background. It is sometimes possible to identify events of an anthropogenic origin among them—light of cities, industrial sites, airports, etc. These events have strongly non-uniform illumination of the focal plane. A frequency modulation of the signal at 100 Hz or 120 Hz is observed for such events in case they are registered with a temporal resolution of 0.4 ms.

Another major group of events ( $\sim 14\%$ ) represents instant (i.e., happening in one or, rarely, two time samples of  $0.8 \mu\text{s}$ ) and usually intensive flashes that produce tracks or, sometimes, small spots in the focal surface. An example is shown in Fig. 1. Preliminary simulations [4] performed with the Geant4 framework [5] and the geographical distribution of the events support the hypothesis that they are due to charged particles passing through the UV glass filters and PMTs of the focal plane. A detailed analysis is in progress.

Another group of events registered in the EAS mode consists of records with monotonously increasing ADC counts with comparatively slow rise time ( $100 \mu\text{s}$ ). Such flashes typically evolve simultaneously in the majority of pixels presenting an almost uniform illumination of the focal plane. An analysis of the geographical distribution of the flashes and their comparison with data from the World-Wide Lightning Location Network (WWLLN) provide evidence for their close relation to simultaneous thunderstorm activity, possibly far from the FOV of TUS.

TUS has also registered a few events that are likely to be elves—short-lived optical phenomena that manifest themselves at the lower edge of the ionosphere as bright rings expanding at the speed of light up to a maximum radius of  $\sim 300$  km [6]. An event presented in Fig. 2 was registered on September 18, 2016, above Africa ( $9^\circ 7' \text{N}$ ,  $17^\circ 1' \text{E}$ ) at 22:06:48 UTC. The record demonstrated an arc-like track that crossed the focal plane approximately at the speed of light. Remarkably, the Vaisala Global Lightning Dataset GLD360 [7, 8] registered six lightning discharges in the direction to the center of the arc within 1 s from the TUS event, with the closest of them in around

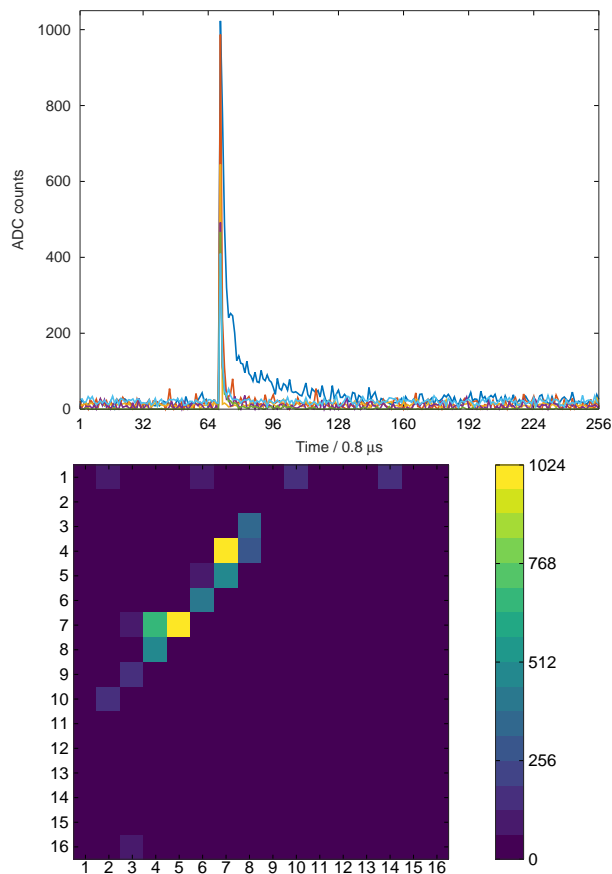


FIG. 1: Example of a track-like event. Top: waveforms of six PMTs with the biggest ADC counts. Colours denote different pixels. Bottom: snapshot of the focal surface at the moment of the peak. Colours denote real ADC counts.

$\sim 130$  km from the center of the TUS FOV. The direction to the lightnings and the geometry and dynamics of the signal support the elve hypothesis.

Numerous thunderstorm events were registered in the TLE mode of operation with the time sampling of 0.4 ms. These events have diverse spatial dynamics and temporal structures with multiple peaks and complicated shapes. Some of them cause signal in all pixels, others demonstrate a clear structure with non-uniform illumination of the focal plane and an obvious center of the event. These events were compared with data of the WWLLN and the Vaisala GLD360. An example is shown in Fig. 3. It was recorded on June 27, 2016, above India ( $25^\circ 3' \text{N}$ ,  $77^\circ 8' \text{E}$ ). Not seen in the figure, the event had complicated temporal and spatial dynamics. Several lightning strikes were registered by the Vaisala GLD360 in this region at the moment of the event, and two of them took place exactly in the FOV of TUS.

As we have stated above, the search for an EAS born by an extreme energy cosmic ray is the priority goal of the TUS experiment. As of January, 2017, we have not found strong candidates for EAS events in

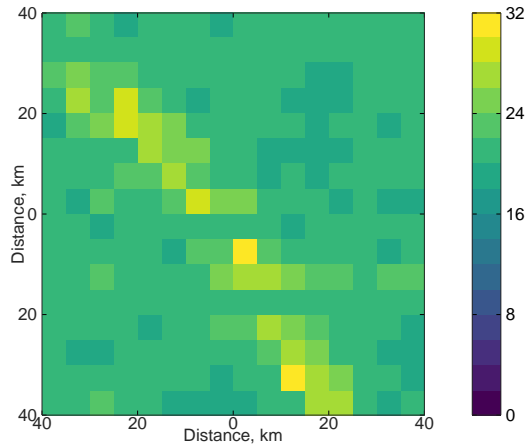


FIG. 2: Snapshot of the focal plane for an elve registered on September 18, 2016. ADC counts are scaled to individual PMT gains. Geographic North is approximately at the top of the plot. Numbers along the axes denote distance from the center of the FOV at sea level.

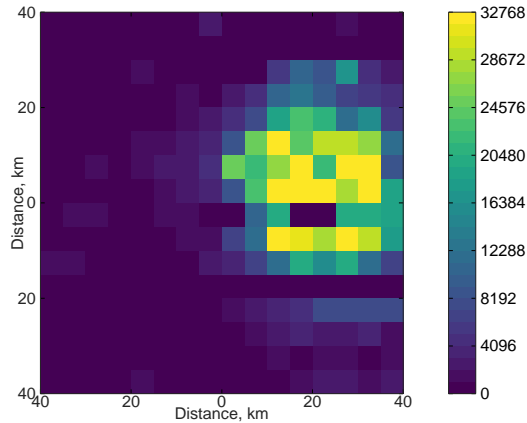


FIG. 3: Snapshot of the focal plane for an event registered of June 27, 2016, above India. Colours denote real ADC counts.

the TUS data but an intensive study is in progress.

### III. GRB OBSERVATIONS ON BOARD LOMONOSOV

A study of GRBs is one of the main goals of the Lomonosov space mission. The Lomonosov satellite is the first space mission in which the multi-wave-length observations of GRBs are realized in real time without necessity of an optical instrument re-orientation on a GRB monitor trigger. The mission payload includes the GRB monitor BDRG, wide-field optical cameras SHOK and the UFFO (Ultra-Fast Flash Observatory) instrument consisting of the X-ray imaging UBAT telescope and the UV slewing mirror telescope SMT. The SHOK cameras are placed in such a way that their fields of view are overlapped by the GRB

monitor detector FOV. This allows simultaneous GRB observations in gammas and optics in all-time scale of event evolution including obtaining optical light curves of prompt emission as well as of precursors. The real time data transfer in the Gamma-ray Coordinates Network (GCN) of detected GRB is realized, as well as operative control of BDRG data on triggers from ground based facilities including neutrino and gravitational wave detectors.

The BDRG gamma-ray spectrometer is designed to obtain the temporal and spectral information of GRBs in the energy range of 10–3000 keV and to provide GRB triggers on several time scales (10 ms, 1 s and 20 s) for ground and space telescopes, including UFFO and SHOK. The BDRG instrument consists of three identical detector boxes with axes shifted by  $90^\circ$  from each other. This configuration allows us to localize a GRB source in the sky with an accuracy of  $\sim 2^\circ$ . Each BDRG box contains a phoswich NaI(Tl)/CsI(Tl) scintillator detector. Data from the three detectors are collected in an information unit, which generates a GRB trigger and a set of data frames in the output format. The scientific data output is  $\sim 500$  Mb per day, including  $\sim 180$  Mb of continuous data for events with duration in excess of 100 ms for 16 channels in each detector, detailed energy spectra, and sets of frames with  $\sim 5$  Mb of detailed information for each burst-like event. A number of pre-flight tests including those for the trigger algorithm and calibration were carried out to confirm the reliability of the BDRG for operation in space.

Another instrument consists of two fast, fixed, very wide-field SHOK cameras. The main goal of this experiment is the GRB optical emission registration before, synchronously, and after the gamma-ray emission. The FOV of each camera is placed in the gamma-ray burst detection area of other devices located onboard Lomonosov. SHOK provides a registration of optical emissions with a magnitude limit of 9–10<sup>m</sup> on a single frame with an exposure of 0.2 s. The device is designed for continuous sky monitoring at optical wavelengths in the very wide field of view (1000 square degrees each camera), detection and localization of fast time-varying (transient) optical sources on the celestial sphere, including provisional and synchronous time recording of optical emissions from the gamma-ray burst error boxes, registered by the BDRG device and implemented by a control signal (alert trigger) from the BDRG. The core of each SHOK camera is a fast-speed 11-Megapixel CCD. Each of the SHOK devices represents a mono-block, consisting of a node for registration of optical emission, the electronics node, elements of the mechanical construction, and the body.

The primary aim of UFFO/Lomonosov is to capture the rise phase of the optical light curve, one of the least known aspects of GRBs. Fast response measurements of the optical emission of GRBs are to be

made by SMT, which employs a rapidly slewing mirror to redirect the optical axis of the telescope to a GRB position prior determined by the UFFO Burst Alert Telescope (UBAT), the other onboard instrument, for the observation and imaging of X-rays.

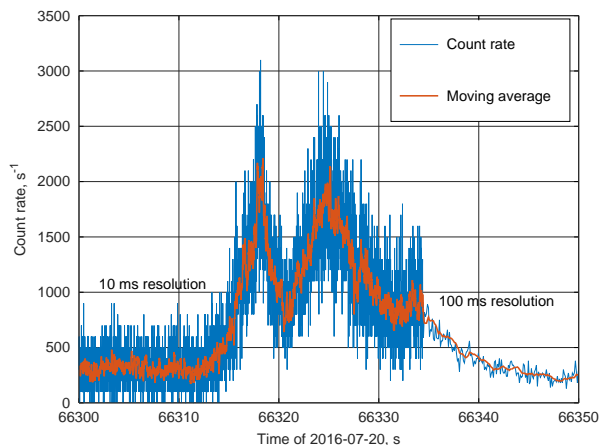


FIG. 4: Time profile of the count rate in the NaI(Tl) 20–170 keV range of the BDRG-2 detector for GRB 160720A.

The main role of UBAT is to monitor the X-ray sky, rapidly capture any source illumination and movement, calculate the source location, and then trigger SMT to observe the early UV/optical counterpart. To detect X-rays, UBAT utilizes a scintillation detector composed of a  $6 \times 6$  array of modules of Yttrium Oxyorthosilicate crystals arranged in an  $8 \times 8$  pixel array, and multi-anode photo multiplier tubes. It uses the well-known coded aperture mask technique to estimate a direction vector of a GRB source in its FOV. All functions are written in the Field Programmable Gate Array firmware to enable fast triggering and imaging algorithms.

Seventeen GRBs were detected and confirmed by other experiments up to January, 2017 (see [https://downloader.sinp.msu.ru/grb\\_catalog/](https://downloader.sinp.msu.ru/grb_catalog/)). GCN circulars were published for all these GRBs. The

smaller than expected number of detected bursts is due to the reduced time for real observations caused by the satellite testing operations that were performed during the initial stage of operation. This also explains the gaps in our data. The time profile of gamma quantum counts of one of the GRBs detected by the BDRG instrument is presented in Fig. 4. Apart from the 17 observed GRBs, the BDRG instrument has detected six bursts from the magnetar SGR1935+2154 as well as a few solar flares at X- and gamma rays.

The main advantages of the BDRG instrument in comparison with the Konus-Wind experiments [9] are the possibility of gamma by gamma reading for detected events and the use of phoswich detectors, which allow effective separation of gamma quanta from electrons. The possibility of such a distinction provides an opportunity to the GRB search as a result of the elimination of electron precipitation-like events that might otherwise be mistaken for GRBs. In comparison with other modern GRB experiments, for example the Fermi Gamma-ray Burst Monitor [10], the BDRG payload has comparable sensitivity and temporal resolution, although a slightly smaller effective area. Because of the possibility of operative GRB data transfer via the Globalstar network to the GCN, the BDRG GRB monitor provides a good input to contemporary GRB observations.

### Acknowledgments

The TUS experiment team thanks Robert Holzworth, the head of the World Wide Lightning Location Network, and Vaisala Inc. company for providing data employed in the present study. The work was done with partial financial support from the Russian Foundation for Basic Research grants No. 15-02-05498-a and No. 16-29-13065. The Korean work is supported by the National Research Foundation grants No. 2015R1A2A1A01006870 and No. 2015R1A2A1A15055344.

- 
- [1] V. A. Sadovnichiy, A. M. Amelyushkin, V. Angelopoulos, et al., *Cosmic Research* **51**, 427 (2013), ISSN 1608-3075.
  - [2] B. A. Khrenov, M. I. Panasyuk, V. V. Alexandrov, et al., in *Observing Ultrahigh Energy Cosmic Rays from Space and Earth*, edited by H. Salazar, L. Vilasenor, and A. Zepeda (2001), vol. 566 of *American Institute of Physics Conference Series*, pp. 57–75.
  - [3] B. A. Khrenov, M. I. Panasyuk, G. K. Garipov, et al., in *European Physical Journal Web of Conferences* (2013), vol. 53, p. 09006.
  - [4] G. K. Garipov, M. Y. Zotov, P. A. Klimov, et al., *Bull. Rus. Acad. Sci. Physics* **81**, 407 (2017).
  - [5] S. Agostinelli, J. Allison, K. Amako, et al., *Nuclear Instruments and Methods in Physics Research A* **506**, 250 (2003).
  - [6] H. Fukunishi, Y. Takahashi, M. Kubota, et al., *Geophysical Research Letters* **23**, 2157 (1996).
  - [7] R. K. Said, U. S. Inan, and K. L. Cummins, *Journal of Geophysical Research (Atmospheres)* **115**, D23108 (2010).
  - [8] R. K. Said, M. B. Cohen, and U. S. Inan, *Journal of Geophysical Research (Atmospheres)* **118**, 6905 (2013).
  - [9] E. P. Mazets, R. L. Aptekar, S. V. Golenetskii, et al., *Sov. J. Exp. Theor. Phys. Letters* **96**, 544 (2012).
  - [10] C. Meegan, G. Lichti, P. N. Bhat, et al., *Astrophys. J.* **702**, 791-804 (2009), 0908.0450.